

Ultracold Interactions between Ions and Polar Molecules

Leon Karpa¹

¹ Leibniz Universität Hannover, Institut für Quantenoptik, 30167 Hannover, Germany

Olivier Dulieu²

² Université Paris-Saclay, CNRS, Laboratoire Aimé Cotton, Orsay 91400, France

E-mail: karpa@iqo.uni-hannover.de

Abstract. We discuss a platform for observing and controlling the interactions between atomic ions and a quantum gas of polar molecules in the ultracold regime. This approach is based on the combination of several recently developed methods in two so-far complementary research domains: ion-atom collisions and studies of ultracold polar molecules. In contrast to collisions between ions and ground-state atoms, which are dominated by losses due to three-body recombination (TBR) already at densities far below those typical for quantum degenerate ensembles, our proposal makes use of polar molecules, their rich level structure, and sensitivity to electric fields to design effective interaction potentials where ion-neutral TBR losses and molecule-molecule losses due to sticky collisions are strongly suppressed. This may enable access to the deep quantum regime of interaction with a broad range of applications including the potential formation of novel many-body self-bound states, quantum simulations, and quantum chemistry between polyatomic molecules.

ion-atom interactions, molecular quantum gases, quantum chemistry, many-body physics

1. Introduction

Controlling collisions between ions and neutral atoms in a regime where quantum effects are dominant is a long-standing goal in the field of ion-atom interactions [1–3]. This comparatively new and interdisciplinary research domain holds great promise in advancing or enabling a broad spectrum of applications in areas including quantum many-body and polaron physics [4–7], charge mobility [8, 9], quantum simulations (QS) [10, 11], quantum chemistry (QC) [12–17], and quantum information processing (QIP) [18–20]. Most of these applications either strongly benefit from or require ultralow temperatures where collisional processes are dominated by the contribution of the lowest partial wave, the so-called s-wave regime. During the last years, enormous progress has been made towards this goal. In particular, recent advances have enabled several key achievements such as the elimination of micromotion-induced heating in generic compound optical traps [21], sympathetic cooling below the Doppler limit and close to the s-wave regime [17, 21, 22], and the controlled association of ion-atom Feshbach molecules [17].

However, some substantial challenges remain an obstacle in view of many envisioned applications which require access to the deep quantum regime characterized by a combination of quantum degenerate atomic gases and ions in or close to the motional ground state. This is largely due to inelastic or reactive collisions which dominate already at moderate neutral densities [21, 23, 24] even for spin-polarized fermionic ensembles [17, 22] and lead to loss of the ion. They originate from the comparatively large characteristic range of the interaction potential of typically $R^* \sim 100$ nm between an electric charge and the induced dipole moment of the atoms exposed to the electric field of the ion. For ground-state atoms located at the distance R from the ion, this attractive interaction potential scales as $1/R^4$ and manifests itself in the form of strong enhancement of ion-atom-atom three-body recombination processes (TBR) [23, 25–27]. At the same time, the attractive interaction is also responsible for a displacement of the ion from the node of the radiofrequency (rf) quadrupole field used to generate the confining potential for the ion, facilitating energy transfer from the rf field to the center of mass motion of the ion-atom system whenever they are allowed to undergo collisions [28].

This so-called micromotion-induced heating has been identified as one of the principal obstacles to reaching the s-wave regime in conventional hybrid traps utilizing rf fields to confine the ions [28]. In order to circumvent these limitations, several strategies have been brought forward making use of different systems and mechanisms such as Rydberg atom-atom interactions [29, 30], Rydberg dressing [31], restricting the studies to few specific combinations with an extremely low reduced mass [17, 22, 28], and bichromatic traps for confining ion and atoms [21, 32]. While all these strategies have enabled recent breakthroughs, the combination of ions with quantum degenerate atomic ensembles which are characterized by large phase-space densities on the order of 1 and comparatively high densities of typically $n \sim 10^{15} \text{ cm}^{-3}$, is still out of reach. This is a consequence of the strong enhancement of TBR in vicinity of an ion in conjunction with the scaling of the related loss rates as n^2 resulting in drastically reduced ion lifetimes expected for the required densities [17, 21, 23].

In parallel to the rapid evolution of studies focusing on ion-atom combinations, the complementary field of molecular quantum gases has seen a similarly impressive development. While the focus of the field shifted from chemically reactive alkali mixtures investigated in first ground-breaking experiments [33, 34] to nonreactive combinations and directly laser cooled molecular species, the surprisingly limited lifetimes observed for all species emerged as one of the main challenges. For non-reactive combinations, the underlying losses have prevented the implementation of evaporative cooling, and until recently, hampered the creation of quantum degenerate gases. The exact mechanism behind these losses remains unclear and is a subject of ongoing debates [35, 36], but it is likely related to so-called sticky collisions, which occur at short intermolecular distances and involve the formation of metastable collisional complexes [35–38]. With the development of methods to prevent the molecules from reaching the short range [39–43], this obstacle has recently been overcome [44, 45]. Such shielding methods rely on engineered potential barriers created through interactions with microwave, optical or static electric fields. They have enabled efficient evaporative cooling [46–48], and the first observations of molecular Fermi gases [46, 49] and Bose-Einstein Condensates (BECs) [48] have now become a reality.

Here, we discuss the possibility to combine

the methodology and advantageous properties of the respective systems employed in both fields in order to extend experimental studies of ion-molecule interactions at ultralow temperatures towards quantum gases of polar molecules. First, we give a brief overview of the recent developments in the fields of ultracold molecules and ion-atom interactions, discuss how existing techniques can be used to realize a suitable hybrid platform, and derive the expected properties and behavior of polar molecules exposed to the electric field of a stationary ion. In the subsequent sections, we investigate how the gain of additional degrees of freedom and the resulting interplay of attractive and repulsive long-range and short-range interactions can be used to engineer mechanisms for suppressing undesired processes, both in dilute and in dense ensembles of polar molecules. Lastly, we discuss potential applications of the proposed hybrid ion-molecule system in studies of quantum-chemical reactions, many-body phenomena, and dynamical processes in molecular quantum gases as well as their control.

2. Experimental toolbox for hybrid trapping of ions and neutral molecules

Modern experiments capable of producing ultracold ground-state bialkali molecules follow a route building upon methodology developed for the preparation of quantum degenerate atomic gases, extended to facilitate a combination of two species in the same apparatus. This typically involves Zeeman slowing of thermal beams and subsequent laser cooling, magneto-optical, magnetic, and optical trapping followed by evaporative cooling (close) to quantum degeneracy. The final steps include the association of loosely-bound molecules by exploiting magnetically tunable Fano-Feshbach resonances, and finally, the controlled transfer to the rovibronic ground state via stimulated Raman adiabatic passage (STIRAP), a coherent two-photon process. When considering the part required for the creation of an ultracold ensemble, a typical molecule apparatus incorporates additional layers of complexity compared to an experimental setup designed for trapping and manipulation of a single atomic species. Nonetheless, several experiments have succeeded in preparing and controlling ensembles of ground-state molecules, with the achievement of quantum-degenerate molecular gases marking a milestone in the development of the field [46, 48, 49]. Despite the additional complexity, such experiments can be realized in a laboratory environment that is comparable to that of single-species machines.

In parallel to these developments in the field of ultracold molecular gases, first experiments for

studying ultracold ion-atom collisions have been realized [12, 13]. Their aim was to combine vastly different methodologies for preparing and controlling atoms and ions at ultralow temperatures in a common two-species apparatus. Such hybrid setups using radiofrequency (rf)-driven Paul traps to confine ions and (magneto-) optical traps for preparing and controlling ultracold atomic ensembles have proven to be a versatile platform and have been successfully demonstrated for many ion-atom combinations [12–14, 16, 17, 22, 24, 50–56]. More recently, it was shown that this concept can be extended to combinations of several species of atomic ions and multi-species atomic magneto-optical traps which can be used to study ion-atom collisions at low temperatures and in principle support the association of bialkali molecules [56]. Among the many important developments in this field, we point out two specific examples that are most relevant in view of the proposed extension of the study of ion-neutral interactions to ensembles of molecular quantum gases, that is, highly optimized rf-based hybrid traps and all-optical ion-atom traps. In the former case, for favorable ion-atom combinations featuring low reduced mass and long-range induction coefficients, optimized Paul traps in conjunction with advanced schemes for the detection and compensation of stray electric fields have allowed to reduce the collision energy to a range where non-classical effects become visible [17, 22]. In the latter case, similarly optimized setups were also combined with bichromatic optical traps capable of simultaneously confining ions and atoms [21, 32]. In particular, using optical traps provides the advantage that micromotion-induced heating can be completely eliminated and that this method is applicable to generic combinations of species provided that an effective optical trapping potential can be engineered [57]. In principle, this is the case for any combination of ions and neutral atoms or molecules possessing a non-zero dipole moment.

In addition to ensembles of bialkali molecules such as those given in Table 1, the same concept can be applied to experiments on the level of individual particles, e.g. single molecules in optical tweezers [58–61] and to other classes of polar molecules, e.g. directly laser-coolable CaF [61–63] and BaF [64], NaCs [58], RbCs [59], and polyatomic molecules such as CaOH [60] or CaOCH₃ [65]. For clarity, we will focus our discussion on the exemplary ensembles of ground-state NaK and Ba⁺ ions for the following reasons. Firstly, molecular quantum (-degenerate) gases with a high phase-space density have been recently achieved for NaK [46, 66], and secondly, both the ions and the molecules can be routinely confined and prepared in standard optical dipole traps [46, 66–70]. Furthermore, as we will discuss in the remainder of this section, NaK

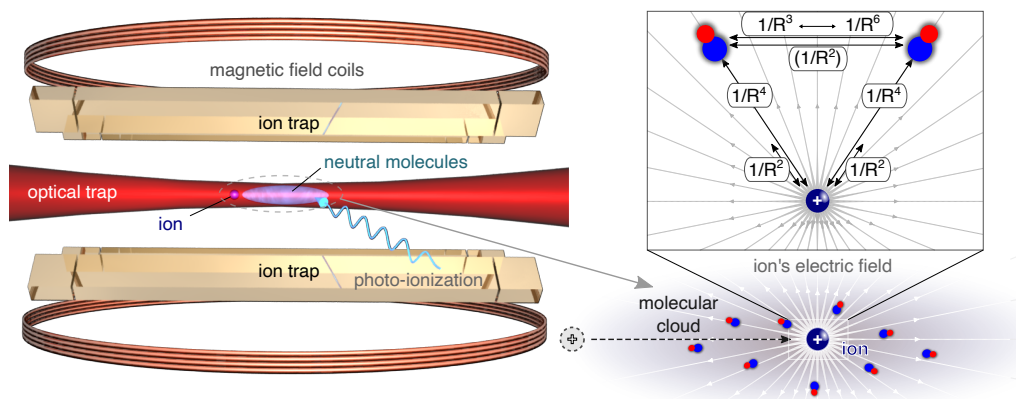


Figure 1. (a) Schematic of an ion-molecule hybrid trap combining a magnetic trap, optical dipole traps, and an integrated trap for ions for investigating and controlling the interactions between single ions and neutral molecular quantum gases. (b) An ion immersed into the neutral cloud introduces a source of static electric fields, aligning the permanent molecular electric dipoles, depending on the distance R . This provides access to a new system with a rich hierarchy of competing tunable interactions spanning $1/R^6$ (induced dipole – dipole, attractive), $1/R^4$ (charge – induced dipole, attractive or repulsive: depending on the quantum numbers J, m_J), $1/R^3$ (dipole – dipole, attractive for side-by-side or repulsive for head-to-tail collisions), $1/R^2$ (charge – dipole, attractive or repulsive: determined by the electric field and J, m_J). The transition from the $1/R^4$ to the $1/R^2$ potential occurs above the characteristic electric field \mathcal{E}^* .

molecules prepared in the rovibronic $^1\Sigma^+$ ground state have very similar properties to common alkali species regarding mass and dynamic dipole polarizability $\alpha_d(\omega)$ with ω denoting the frequency of the interacting optical field. This allows for detailed comparisons of the expected behavior of the proposed ion-molecule system with $\text{Ba}^+\text{-Rb}$ mixtures which have been extensively studied both in presence of micromotion-induced heating encountered in rf-hybrid [23–25] and in fr-free optical traps where micromotion is eliminated [21]. Lastly, near-infrared (NIR) far-off resonant optical traps operated at a wavelength of 1064 nm, have been successfully used both to trap NaK and to demonstrate a generic approach to studying ion-atom collisions, first realized for $\text{Ba}^+\text{-Rb}$ mixtures [21]. To this end, bichromatic optical potentials are created by overlapping dipole traps of different wavelengths.

For a direct comparison with previous experiments we use the parameters employed in [21], that is, optical dipole traps with wavelengths of 532 nm (VIS ODT) and 1064 nm (NIR ODT), optical powers $P_{\text{VIS}} = 0.47$ W and $P_{\text{NIR}} = 0.13$ W (adjusted for typical temperatures of NaK quantum gases), matched $1/e^2$ waist radii $w_0^{\text{VIS}} = w_0^{\text{NIR}} = 3.8 \times 10^{-6}$ m, a residual stray electric field of $\mathcal{E}_{\text{str}} = 10$ mV m $^{-1}$, and the axial secular frequency of the linear Paul trap of $\omega_x/(2\pi) = 12$ kHz, respectively. We then calculate the bichromatic potential suitable for overlapping a barium ion laser cooled close to the Doppler temperature $T_D^{\text{Ba}} = 365$ μK with an ensemble of ground-state NaK molecules prepared at $T^{\text{NaK}} = 400$ nK. The NaK molecules experience a repulsive potential from the VIS ODT due to its blue detuning with respect to the energetically lowest dipole-allowed optical transition

$X^1\Sigma^+ \leftrightarrow A^1\Sigma^+$. To maintain the initial trap depth $U_0^{\text{NaK}}/(k_B) \approx 4$ μK , the intensity of the NIR ODT has to be increased compared to its initial value in order to achieve the desired differential light shift. Despite the substantially more complex energy level structure of molecules in comparison with alkali atoms, the resulting potentials calculated in the far-off-resonant limit [71] and using the dynamic dipole polarizability of NaK [72], that are shown in Fig.2 are quantitatively very similar to those obtained for the previously demonstrated case of $\text{Ba}^+\text{-Rb}$ in terms of trap depths and ODT parameters. This suggests that the protocols for overlapping ions and atoms demonstrated in [21] as well as proposed methods for further improving the trapping performance and realizing more complex trapping configurations [57, 69, 70] are readily applicable to molecules. The expected compatibility to such an extent may seem surprising at first glance because, in general, neutral atoms and polar molecules may have vastly different polarizabilities. This is indeed the case for the static polarizability α_0 which is a pivotal point of the proposed experiments and is discussed in detail in section 3. However, in the optical and near-infrared frequency domains where the detunings with respect to rotational transitions are several orders of magnitude larger than those for optical transitions, all $\alpha_d(\omega)$ for the bialkali molecules in the rovibronic ground state as listed in Table 1 vary by less than a factor of 2 and are of the same order of magnitude as those of common alkali atoms [72]. It is this robustness of the dynamic polarizability that facilitates the creation of molecules from individually prepared atomic species which are typically all confined in the

same far-detuned optical dipole traps. At the same time, even within the same electronic and vibrational ground state manifold, i.e. $|X^1\Sigma^+, v=0\rangle$, $\alpha_d(\omega)$ exhibits a substantial dependence on the rotational quantum numbers J and m_J [73].

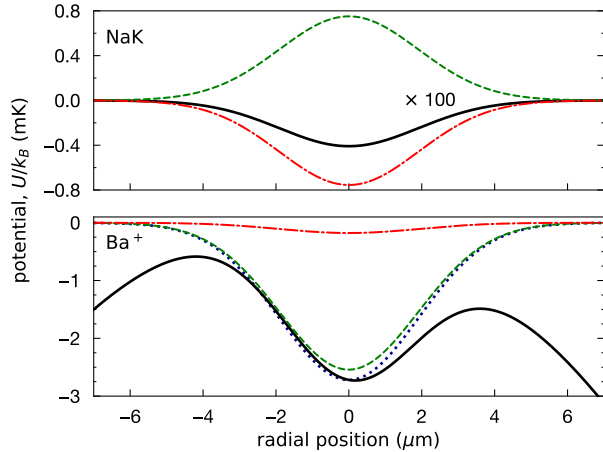


Figure 2. Effective bichromatic radial (orthogonal to the ODT’s wavevector) potentials (black solid lines) for Ba^+ (in the electronic ground state $6^2S_{1/2}$) and NaK (in the rovibronic ground state $|X^1\Sigma^+, v=0, J=0\rangle$) exposed to a composite optical dipole trap superimposing ODTs at 1064 nm (NIR, red dashed-dotted line) and at 532 nm (VIS, green dashed line). The effective potential of NaK is enlarged by a factor of 100 for visibility. The Paul and optical dipole trap parameters are adopted from experiments with Ba^+ -Rb mixtures, accounting for the properties of NaK at a temperature of $T^{\text{NaK}} = 400$ nK.

Exploiting the similarities between molecules and alkali atoms interacting with far-detuned optical fields, a prototypical experimental setup could be realized as shown in Fig.1. Its central features include (i) a Paul trap optimized for ion-neutral experiments, that is, optical access through high numerical aperture objectives beneficial for stray electric field compensation and focusing of the dipole trap beam(s) and the correspondingly designed ion-electrode spacing (~ 1 mm), (ii) magnetic field coils required for the magneto-association of Feshbach molecules, as well as (iii) a bichromatic optical dipole trap. Similar Paul traps have been demonstrated and feature suppression of stray electric fields down to $\sim 10^{-3}$ V m $^{-1}$ [17, 21, 70, 74], very low anomalous heating rates [68], and typical trap depths on the order of $k_B \times 10^4$ K, which is sufficiently deep to recapture ionic products.

The above considerations suggest that the proposed hybrid platform is suitable for investigations of ultracold ion-molecule interactions, such as precise studies of controlled quantum chemistry which are discussed in section 4. In the following sections, we focus on the expected behavior of the system and discuss

Table 1. Characteristic properties of the charge-induced dipole long-range interaction between common heteronuclear bialkali molecules prepared in the rovibronic ground state and a $^{138}\text{Ba}^+$ ion. The static dipole polarizabilities α_0 and permanent electric dipole moments (PDM) are taken from [72]. For comparison, ^{87}Rb and ^6Li are given as a reference for ion-atom systems, representing a typical and one of the most favorable combinations with respect to reaching the s-wave scattering limit, respectively.

	PDM (D)	α_0 (10^{-37} C m 2 V $^{-1}$)	R^* (10^{-6} m)	E^*/k_B (nK)
LiCs	5.59	312	25.9	0.00521
NaCs	4.69	709	40.1	0.00206
LiRb	4.18	152	16.2	0.0165
LiK	3.58	93.6	10.0	0.0703
NaRb	3.31	294	23.6	0.00711
NaK	2.78	152	14.2	0.0281
KCs	1.84	208	22.2	0.00644
RbCs	1.25	177	21.6	0.00614
KRb	0.62	18.8	6.21	0.0952
LiNa	0.57	1.64	1.12	7.86
Rb	0.00	0.0526	0.295	52.3
Li	0.00	0.0270	0.0694	8760

several potential applications of the proposed hybrid platform.

3. Polar molecules in the electric field of an atomic ion

Firstly, we consider the situation where an ion is approached by a single polar molecule prepared in its rovibronic ground state at a given distance R . In this situation, the charge-dipole interaction of each individual molecule in the $^1\Sigma^+$ ground state with the ion is determined by the Stark effect [75]:

$$\hat{H}_{CD} = -\vec{d}(\vec{\mathcal{E}}) \cdot \vec{\mathcal{E}}(R), \quad (1)$$

with matrix elements $\langle J, m_J | -\vec{d}(\vec{\mathcal{E}}) \cdot \vec{\mathcal{E}}(R) | J', m'_J \rangle$ for any two states $|J, m_J\rangle$ and $|J', m'_J\rangle$ coupled by \mathcal{E} at a distance R from the ion. The resulting mixing of rotational states with different parity gives rise to a finite permanent dipole moment in the ion-molecule center of mass frame.

The rovibrational spectrum at zero field is approximated by the Dunham series:

$$U_{rov} = \sum_{lk} Y_{lk} \left(v + \frac{1}{2}\right)^l J^k (J+1)^k, \quad (2)$$

where Y_{lk} denote the Dunham coefficients and the indexes l, k the powers of the vibrational and rotational quantum numbers v and J [76]. For the vibrational ground state $v = 0$, the rotational energy is approximately $U_{rov} \approx B_0 J(J+1)$, with the rotational constant B_0 . For large ion-molecule separations corresponding to the low-field limit, second order perturbation theory reveals that the shifts of the

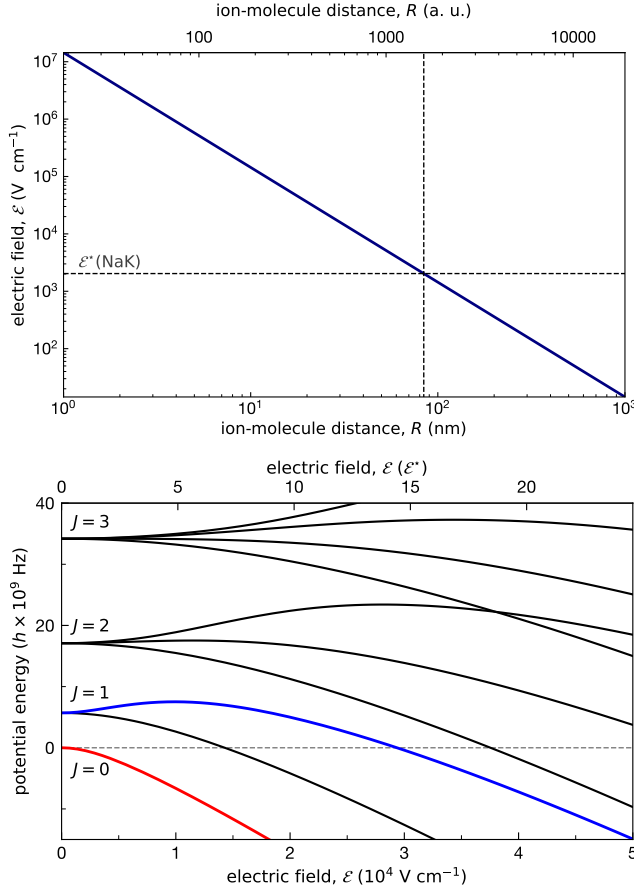


Figure 3. (top panel) Magnitude of the electric field emanating from a single ion as a function of its distance to an approaching neutral molecule. The shaded area indicates the distance range of Fig.5, where charge exchange reactions are exothermic. The corresponding electric potential experienced by the molecules becomes extremely large ($> 100 \text{ kV cm}^{-1}$) resulting in almost complete alignment of the molecular dipole moment ($d(\mathcal{E}) > 0.9 d_0$). The grey dashed line denotes the characteristic electric field of NaK, $\mathcal{E}^*(\text{NaK}) = d_0/B_0 = 2.04 \text{ kV cm}^{-1}$. (bottom panel) Numerically calculated energy levels of the NaK molecule for the lowest rotational states $|J = 0, 1, 2, 3; m_J\rangle$ (considering a maximal $J_{max} = 10$) within the vibronic ground state manifold $|X^1\Sigma^+, v = 0\rangle$ as a function of an external electric field of magnitude \mathcal{E} . The hyperfine structure which is on the order of $h \times 100 \text{ KHz}$ is neglected for simplicity. The lowest high and low-field seeking states (up to $\mathcal{E} \approx 5 \mathcal{E}^*$), $|J = 0, m_J = 0\rangle$ and $|J = 1, m_J = 0\rangle$, are shown as red and blue solid lines, respectively.

eigenvalues $U_{CD}(\mathcal{E})$ of \hat{H}_{CD} are quadratic in \mathcal{E} . In this regime, expanding U_{CD} to second order in \mathcal{E} , we obtain:

$$U_{CD}(\mathcal{E}) = U(\mathcal{E}) - d(\mathcal{E})|_{\mathcal{E}=0} \mathcal{E} - \frac{1}{2} \alpha(\mathcal{E})|_{\mathcal{E}=0} \mathcal{E}^2 + O(\mathcal{E}^3), \quad (3)$$

with the induced dipole moment and static polarizability being:

$$d(\mathcal{E}) = -\frac{\partial U_{CD}(\mathcal{E})}{\partial \mathcal{E}}, \quad \alpha(\mathcal{E}) = -\frac{\partial^2 U_{CD}(\mathcal{E})}{\partial \mathcal{E}^2}.$$

As an example, these quantities are shown for the rovibronic ground state $|X^1\Sigma^+, v = 0, J = 0, m_J = 0\rangle$ of NaK in Fig.4, for the corresponding eigenvalue from Fig.3. The characteristic electric field $\mathcal{E}^* = B_0/d_0$ marks the transition from the weak-field to the strong-field regime. For example, in NaK this occurs at $\mathcal{E}^* = 2.04 \text{ kV cm}^{-1}$. For $\mathcal{E} \rightarrow 0$, the linear curvature of U_{CD} is negligible and d vanishes, whereas α is maximal and the energy shifts are dominated by the quadratic Stark effect. Considering this weak-field limit (valid for $\mathcal{E} < \mathcal{E}^*$) and utilizing the ion with an electric charge q as a point-like source of an external electric field $\mathcal{E} = q/(4\pi\epsilon_0 R^2)$ for the surrounding molecules, we obtain the long-range ion-molecule potential

$$U_{CD}(R)|_{R \rightarrow \infty} = -\frac{1}{2} \alpha_0 \mathcal{E}^2 = -\frac{1}{2} \frac{\alpha_0 q^2}{(4\pi\epsilon_0)^2} \frac{1}{R^4}. \quad (4)$$

where the vacuum permittivity is denoted by ϵ_0 . This can be interpreted in the following way. While polar molecules possess a permanent electric dipole moment

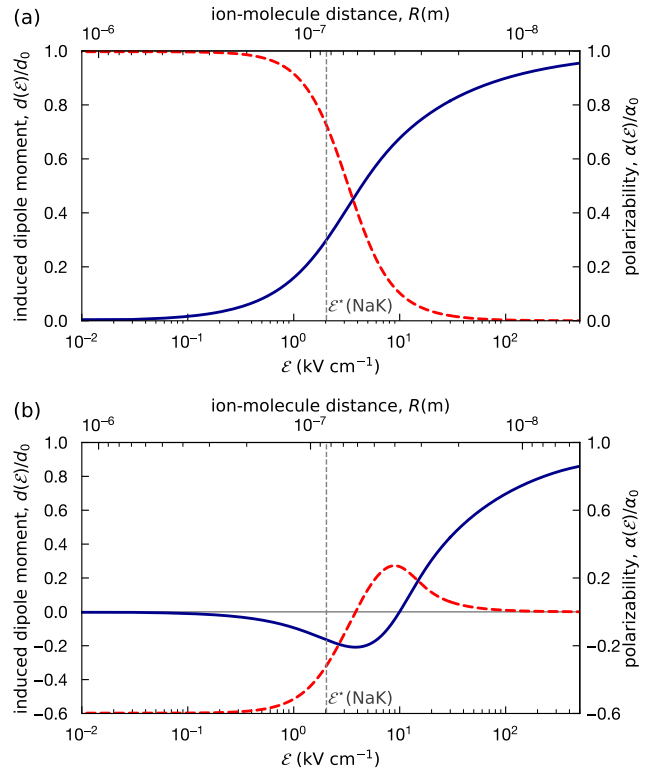


Figure 4. Induced dipole moment $d(\mathcal{E})$ (blue solid line) and the static polarizability $\alpha(\mathcal{E})$ (red dashed line) for NaK as a function of the electric field \mathcal{E} created by an ion separated by the distance R from the (stationary) molecule. (a) Calculated $d(\mathcal{E})$ in units of the permanent dipole moment d_0 and $\alpha(\mathcal{E})$ in units of α_0 (taken from [72]) for the rovibronic ground state $|X^1\Sigma^+, v = 0, J = 0, m_J = 0\rangle$ and (b) the $|X^1\Sigma^+, v = 0, J = 1, m_J = 0\rangle$ state. The characteristic electric field $\mathcal{E}^* = B_0/d_0$ is shown as the horizontal dashed line.

(PDM) in their own reference frame, the effective dipole moment in the laboratory frame is zero in absence of an external electric field. Therefore, in the long-range, a molecule exposed to the ion's electric field will acquire an induced dipole moment, giving rise to an attractive potential described by Eqn.4. This result resembles the familiar expression for charge-induced dipole interactions which dominate ion-atom collisions where the long-range induction coefficient is given by $C_4 = \alpha_0 q^2 / (4\pi\epsilon_0)$ [77], and allows us to directly compare the expected long-range behavior of ions immersed into ensembles of polar molecules with the well-explored ion-atom systems. Analogously, we use the following expressions derived from the semiclassical Langevin scattering model [78, 79], to calculate the range of this potential and the characteristic energy scale for s-wave collisions:

$$R^* = \sqrt{2\mu C_4 / \hbar^2} \quad (5)$$

$$E^* = \frac{\hbar^4}{4\mu^2 C_4} = \frac{\hbar^2}{2\mu (R^*)^2}. \quad (6)$$

Here, \hbar and μ denote the reduced Planck's constant and the reduced mass of the ion-neutral system, respectively.

When considering the electronic ground state, one of the most significant features of heteronuclear molecules is that the magnitude of the static polarizability is typically several orders of magnitude larger than that of atoms as summarized in Table 1 for the case of an immersed Ba^+ ion. As pointed out in [72], this enormous enhancement comes about because α_0 varies as the inverse of the energy for the lowest allowed transition from the rotational ground state. While the dipole moment of transitions between rotational states is comparable to that of dipole allowed transitions to electronically excited states, the energy separation of rotational states is of the order $B_0 \sim \hbar \times 10$ GHz. The latter is about five orders of magnitude lower than the energy of typical electronic transitions, such that α_0 and the C_4 coefficients are correspondingly larger. For instance, the combination Ba^+ and NaK, with the latter being prepared in the rovibronic ground state and possessing a PDM in the body-fixed frame of $d_0 = 2.78$ D as well as a static electric dipole polarizability of $\alpha_0 = 9.237 \times 10^5$ a.u. [72], yields the long-range induction coefficient $C_4^{\text{Ba-NaK}} = 1.58 \times 10^{-53}$ C m V $^{-1} \approx 3 \times 10^3 C_4^{\text{Ba-Rb}}$. For the corresponding characteristic range of the interaction and the related energy scale we obtain $R_{\text{NaK}}^* = 14.2 \mu\text{m}$ and $E_{\text{NaK}}^*/k_B \approx 3 \times 10^{-11}$ K. This straightforward result already reveals two principal properties of the expected ion-molecule interactions. Firstly, the range of the charge-induced dipole potential is extremely large compared to the characteristic range of ion-atom interactions which is typically on the order of 100 nm, e.g.,

$R_{\text{Rb}}^* \approx 300$ nm for Rb prepared in its electronic ground state. And secondly, compared to ion-atom mixtures, the related energy threshold for entering the s-wave regime is drastically reduced even further by several orders of magnitude. For comparison, the corresponding s-wave threshold in rubidium is $E_{\text{Rb}}^*/k_B \sim 10^{-8}$ K while the most favorable mixtures such as Yb^+ -Li and Ba^+ -Li feature a much higher threshold on the order of $k_B \times 10^{-6}$ K [28].

In addition to the difficulty of reaching the required extremely low collision energies, another effect potentially poses an even stricter limitation on the range of observable effects: the enhancement of the loss processes due to three-body recombination. From ion-atom collisions it is known that ion-atom-atom TBR becomes the dominant loss process already at comparatively low densities several orders of magnitude below values where atomic ensembles suffer from three-body losses [23], even in the case of spin-polarized fermions [17]. This can be understood intuitively by coarsely estimating the critical density n_C at which the interparticle volume becomes smaller than the active volume $V^* = (4/3)\pi R^{*3}$. The latter is determined by $R^*(n) = (n\mu C_n / (2\hbar))^{1/(n-2)}$ of the dominant interaction $-C_n/R^n$ [79]. For $n > n_C = V^{*-1}$ more than one particle enter V^* at the same time, marking the onset of TBR. In the case of ground-state neutral atoms, R^* arises from the short-range van der Waals potential $-C_6/R^6$. For example, in rubidium $R^* \approx 10$ nm and $n_C = 2.5 \times 10^{17}$ cm $^{-3}$, about two orders of magnitude higher than typical BEC densities. For ground-state atoms colliding with ions, e.g. Rb and Ba^+ , $R^* \approx 290$ nm of the charge-induced dipole interaction $-C_4/R^4$ is about 30 times larger. Therefore, the critical density is already reached at $n_C^{\text{Ba-Rb}} \approx 1 \times 10^{13}$ cm $^{-3}$ which is in agreement with experimental findings [21, 23–25]. For Ba ions interacting with NaK molecules, R^* is once again drastically increased to $R^* = 1.42 \times 10^{-5}$ m, such that V^* would be comparable to the capture volume of typical dipole traps and $n_C^{\text{Ba-NaK}} \approx 1 \times 10^8$ cm $^{-3}$.

Following the analogy to ion-atom interactions, it becomes apparent that reaching the quantum dominated regime in the Ba^+ -NaK system using even the most advanced hybrid platforms is extremely challenging. However, as is the case with ion-atom systems, these results strongly depend on the reduced masses and static polarizabilities of the chosen ion-molecule combination. For example, for Ba^+ -LiNa, the situation is much more comparable to Ba^+ -Rb, with both E^* and R^* being of the same order of magnitude.

In addition to the choice of a suitable combination, all the characteristic properties that are fixed for a given combination of ions and ground-state atoms can

be readily and drastically tuned in polar molecules, including those with an extremely low threshold for s-wave collisions such as NaK and NaCs. Since the polarizability in the relevant limit is simply determined by the second derivative of the potential with respect to \mathcal{E} , we are free to choose any addressable rotational state which will exhibit not only a different magnitude of the polarizability but for particular projections m_J also an opposite character of the polarization potential. For instance, already the first rotationally excited state $|X^1\Sigma^+, v=0, J=1, m_J=0\rangle$ of NaK features a reversed curvature as shown in Fig.4(b). This means that the polarization potential is rendered repulsive and features a barrier with a height of $U_0^{(J=1, m_J=0)}/k_B = 87.4$ mK reached around $\mathcal{E} = 10$ kV cm $^{-1} \approx 5 \mathcal{E}^*$ in NaK as depicted in Fig.3. Therefore, for molecules prepared in this state and at typically achievable temperatures on the order of $T_{mol} \sim 100$ nK $\ll U_0^{(J=1, m_J=0)}/k_B$, we expect that short-range ion-molecule collisions will be strongly suppressed.

In ion-atom systems, conceptually similar ideas for designing effectively repulsive potentials by exploiting Rydberg dressing induced by optical fields have been proposed [31]. In this case, a potential barrier arises from the competition of an engineered repulsive contribution and the attractive static charge-induced dipole potential, both scaling as R^{-4} . In contrast, for molecules interacting with ions, the long range potential itself is repulsive such that the sought-after shielding can be facilitated by exploiting their rich energy level structure, that is, without additional dressing.

This precise control over the rotational degrees of freedom provides a natural mechanism for shielding against inelastic and reactive ion-molecule collisions, opening a way to realize sympathetic cooling. We note, that this expectation holds even in presence of ion micromotion and despite the prediction that E^* in the rovibronic ground state is extremely low compared to the thermal energy of typical molecular quantum ensembles. This intriguing feature hints at the fact that the intuition derived from considering characteristic quantities such as R^* and E^* is only valid for the specific case of molecules prepared in the rovibronic ground state. Furthermore, even in the latter case, the comparison to ion-atom systems only holds in the regime of extremely dilute gases where molecules collide with the ion one at a time, such that the intermolecular interactions are negligible. In contrast, this approximation breaks down for dense molecular gases where the dipole-dipole interactions and many-body effects are expected to play a significant role [80]. This scenario is discussed in section 5.

4. Reactive collisions and formation of molecular ions

One of the most striking features of ion-molecule collisions setting them apart from those between atoms and ions is the much larger static polarizability of heteronuclear molecules, which translates to a drastically lower threshold energy E^* . This means that even at the lowest temperatures on the order of 10 nK that have been observed in molecular systems to date [46,48,81], the collisions of all molecules given in Table 1 with ions would take place in the classical regime. In this limit, the cross section of capture processes is well described by the Langevin model, which predicts $\sigma_L = 2\pi\sqrt{C_4/E}$, where E is the collision energy. The related rate constant for Langevin collisions is independent of E : $K_L = \sigma_L \hbar k / \mu = \pi\sqrt{8C_4/\mu}$. For a direct comparison we consider the interaction of a $^{138}\text{Ba}^+$ ion with $^{23}\text{Na}^{39}\text{K}$ molecules. With the strongly enhanced polarizability of NaK, we expect that the rate for reactive collisions will be enhanced by a factor of $\sigma_L(\text{Ba-NaK})/\sigma_L(\text{Ba-Rb}) \approx 60$.

In ion-atom systems the reactive capture cross sections show a very strong dependence on the electronic state of both the ion and the atomic gas. For example, in collisions between Yb^+ and Li, the loss rates of ions in the states $^2S_{1/2}$, $^2P_{1/2}$, $^2D_{3/2}$, and $^2F_{7/2}$ vary by several orders of magnitude, with the lowest reactivity observed in $^2S_{1/2}$ [82]. Similarly, K_L of $^2S_{1/2}$ Yb ions interacting with Li atoms in the Rydberg state 24S is about 10^3 times larger than for ground-state atoms [83]. In a similar manner, the polarizability of molecules can be manipulated by preparing a specific state $|J, m_J\rangle$. One difference is that these changes are expected without excitation from the electronic ground state or even the vibrational state within the same manifold, that is, they can be brought about with microwave fields. Another distinctive feature is that the rotational states are long-lived compared to electronically excited states. Lastly, the sign of the polarizability itself can be changed by selecting states with specific m_J . The latter means that short-range collisions which are strongly enhanced in the ground state can be suppressed such that using the degrees of freedom offered by the molecules the reactive rates can be tuned from zero to extremely high values comparable to or exceeding those achievable in mixtures of ions and Rydberg atoms.

In order to obtain systems with extremely high chemical reactivity that can be controlled on the quantum level, in addition to a suitably high polarizability, we also require energetically allowed target channels. To investigate if this is the case for the combination of Ba^+ and NaK, we calculate the potential energy surfaces for all combinations of neutral and molecular reactants. As shown in Fig. 5

and 6, we indeed find several open reactive channels. We expect the production of ionic dimers NaK^+ , NaBa^+ , KBa^+ as well as the atomic ions K^+ , Na^+ , Ba^+ and all neutral constituents. This indicates that the system is highly suitable for studies of quantum chemistry at ultralow collision energies. However, the predicted energy release of the exoergic reactions is $\sim k_B \times 10^4$ K. In neutral molecule systems reactions on this energy scale are predominantly signaled by loss. Despite this complication, the rapid development in the field has allowed to obtain much more information about the collisional processes using kinetic energy spectrometry based on photo-ionization in conjunction with velocity-map imaging [84]. This is an example of how combining methodology from complementary fields can provide valuable new insights. In the present case, a hybrid ion-molecule apparatus would be equipped with an integrated Paul trap, such that, in principle, the expected ionic reaction products may be recaptured provided that the trap is suitable for this task. Typical Paul traps, including those employed in hybrid experiments, reach well depths on the order of $\sim k_B \times 10^4$ K [85] which is comparable to the kinetic energy of the expected products. Moreover, the stability region of Paul traps for Ba^+ can be engineered to support the charge-to-mass ratios of the expected product ions which are similar to Rb^+ and Rb_2^+ , species that have been sympathetically cooled by co-trapped Ba^+ [21, 86]. Furthermore, barrierless ion-neutral reactions provide an elegant way to synthesize and study polyatomic molecular ions in

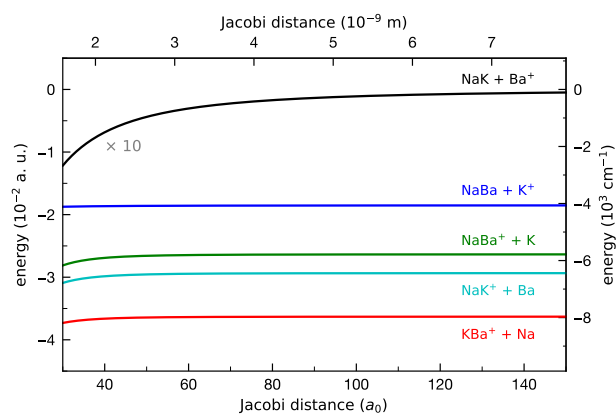


Figure 5. Energies of possible combinations of ionic (and neutral) diatomics (energy taken at the minimum of their ground state PEC) and ground-state neutral atoms (and ions) in a mixture of Ba^+ and NaK (entrance scattering channel), as a function of the ion-molecule (Jacobi) distance R (courtesy of Romain Vexiau). Reactive and charge exchange channels are energetically well separated from the prepared ensemble of Ba^+ and NaK at $R > 60 a_0$ (a_0 : Bohr radius). The long-range variation of the PECs strongly depends on the combination. All energies have been scaled up by a factor of 10 around their asymptotic values for visibility.

hybrid traps [87]. In this regard, similar systems may be realized either in successive ion-molecule collision experiments or by irradiating the ensembles with an ultraviolet photo-ionization beam, in analogy to recent studies of collisions between heteronuclear dimers [84]. Furthermore, it was shown that cooling of ions in a neutral buffer gas is extremely efficient in the classical collision regime and at high energies, even if the ions are not laser-coolable [24, 51]. In our case, ultracold and dense ensembles of three different neutral species, that is Na , K , and NaK can be used for this purpose. Therefore, it is likely that the molecular ions produced in ion-molecule reactions may be recaptured allowing for further manipulation and analysis. This includes sympathetic cooling [88], high-resolution mass spectrometry [86], and (Single shot) Doppler cooling thermometry (SS)DCT [89]. Ultimately, the produced molecules may also be investigated in high-precision measurements based on adapted quantum logic spectroscopy (QLS) methods [90, 91].

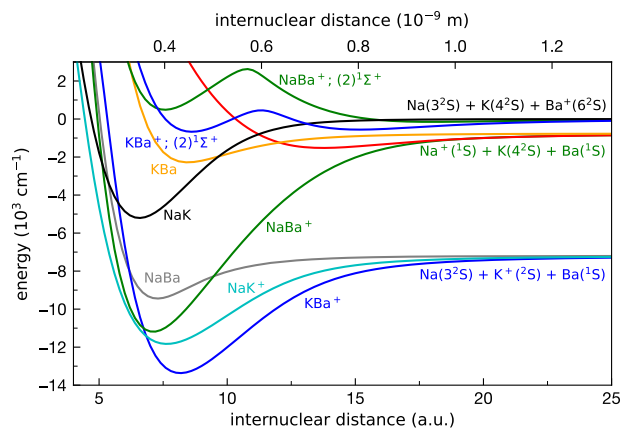


Figure 6. Calculated energies of possible ground state ($X^1\Sigma_g^+$) diatomic molecules composed of Na , K neutral atoms and a Ba^+ ion referenced to the ground-state energy of these three particles. The calculations are performed with the methodology of [72, 92, 93] (courtesy of Romain Vexiau). Note that for completeness we display the second excited state of NaBa^+ and KBa^+ of the same symmetry as they dissociate towards the same limit. The formation of the dimers NaBa^+ , NaK^+ , KBa^+ that are trappable in the same Paul trap as the initially prepared Ba^+ ions is energetically possible. The branching ratios into the different channels as well as the rates of elastic and inelastic collisions strongly depend on the spin and hyperfine states of the constituents and provide a system with rich chemical and collisional properties that can be explored in the proposed setup. The presence of an ion further opens the possibility to control the collisional properties of polar NaK molecules, or NaKBa^+ trimer formation [27], as well as the impact of the ion on the potential creation of NaK - NaK tetramer complexes or, assisted by TBR, ionic pentamers like $\text{Na}_2\text{K}_2\text{Ba}^+$.

5. Ions and high phase-space density polar molecules

Recent experiments capable of reaching ultralow ion-atom collision energies have also enabled first studies of interactions between atomic ions and loosely bound heteronuclear molecules [94]. Taking this concept further to a configuration where ions are immersed into a bath of polar molecules may enable novel polaronic effects due to the important role that the alignment of the molecules is expected to play in the dynamical evolution of such mixtures [80].

In the following we discuss the prospects for such experiments, based on the known properties of collisions between ions and neutral atoms and taking into account the influence of the ion's electric field on the expected effective potentials. So far, we have restricted our configuration to the interaction of an ion with a single molecule prepared in its rovibronic ground state at large distances. In a next step, we will include the impact of the particle density and the internal energy structure of the molecules to derive the expected changes of the interaction potential when approaching the immersed ion.

With the development of methods for the shielding of undesired inelastic collisions, polar molecule experiments are now capable of producing quantum degenerate ensembles [46, 48, 49] with high phase-space and absolute particle densities reaching ~ 1 and 10^{13} cm^{-3} , respectively. Under such conditions, the interparticle distance is typically $\approx 100 \text{ nm}$, which is below the range of charge-induced dipole interactions in the ion-molecule system. As a consequence, the attractive potential will be experienced not by a single molecule but by an ensemble contained within the active volume V^* . We therefore expect that in this situation several molecules will approach the ion at the same time. As an example, for NaK ensembles interacting with a Ba^+ ion $V^*(\text{NaK}) = 1.33 \times 10^{-8} \text{ cm}^3$ such that this scenario occurs at comparatively low densities, e.g. at $n \sim 10^{10} \text{ cm}^{-3}$ on the order of 100 molecules would be addressed simultaneously.

In stark contrast to atoms with zero permanent electric dipole moment, whose collisions with ions are dominated by charge-induced dipole interaction, molecules exposed to the strong field in proximity of the ion become strongly aligned along the electric field axis. Their energy shifts are then dominated by the linear Stark effect. In the radially symmetric electric field, this gives rise to additional contributions to the effective potential due to the repulsive dipole-dipole interaction between pairs of molecules labeled as i, j described by the following Hamiltonian:

$$\hat{H}_{DD} = \sum_{i \neq j} \frac{\hat{d}_i \hat{d}_j (1 - 3 \cos^2(\varphi))}{|\vec{R}_{ij}|^3}, \quad (7)$$

where φ is the angle between the dipole moments $\hat{d}_{i,j}$ and \vec{R}_{ij} the vector connecting the centers of mass of the two molecules.

At distances where $\mathcal{E} \sim \mathcal{E}^*$, the effective dipole moment is a sizable fraction of d_0 and the dominant ion-molecule interaction transitions from the attractive (in the rovibronic ground state) charge-induced dipole potential $-C_4/R^4$ in the long range to $U_{CD} \approx -d_0 \mathcal{E}(R) \propto -d_0/R^2$ in vicinity of the ion where the dipole moments are almost fully aligned with respect to $\vec{\mathcal{E}}$. For example, in rovibronic ground-state NaK molecules the effective dipole moment amounts to $0.67 d_0$ at $\mathcal{E} = 5 \mathcal{E}^*$ as shown in Fig.4. Hence, the effective potential will be determined by the competition between dipole-dipole repulsion and ion-molecule interaction, such that the collective dipole-dipole term which is proportional to d_0^2/R_{ij}^3 will dominate at short range. At the point of equilibrium R_{min} , we expect a local minimum of the effective potential U_{eff} experienced by each molecule of an ensemble contained within the interaction volume V^* of the ion.

To confirm this expectation, we calculate $U_{eff}(R)$ by taking into account the relevant rotationally symmetric ion-molecule and anisotropic dipole-dipole interactions between molecules. For simplicity, we neglect the short-range van der Waals interaction $U_{vdW} = -C_6/R_{ij}^6$, and consider only next-neighbor contributions in an ensemble of N molecules homogeneously distributed on a shell with radius R_{min} centered around the ion, providing a lower bound on the repulsive interaction. We further take into account the finite induced electric dipole moment $d(\mathcal{E}(R))$ of the molecules (as shown in Fig.4) and the finite projection of \vec{d}_i onto \vec{d}_j . The intermolecular distance R_{ij} depends both on R and the total number of molecules as $R_{ij} = 2R \sin(\sqrt{\pi/N})$. Then, the effective dipole moment is $d_{eff}(R) = d(R)(1 - \sin(\sqrt{\pi/N})^2)$. Under these conditions and for an initial density of $n \approx 3 \times 10^{10} \text{ cm}^{-3}$ we obtain the effective radial potential for a single molecule depicted in Fig.7. We find that it indeed exhibits a pronounced minimum with a depth of $U_0/k_B = 56 \text{ mK}$. To confirm that this effect persists with respect to variations of the molecular density, we repeat the calculation as a function of N . The results shown in Fig. 7 indicate that the potential minimum is robust with respect to the number of molecules, with its location shifting towards larger R for higher neutral densities while at the same time the depth is decreasing, as illustrated in Fig.8.

The calculated radial self-bound trapping frequency in the range $N = 300$ to 1000 would be on the order of $\omega_{sb}^{rad}/(2\pi) \sim 10 \text{ MHz}$, e.g. for $N = 350$, $\omega_{sb}^{rad}/(2\pi) \approx 35 \text{ MHz}$ indicating that the molecules

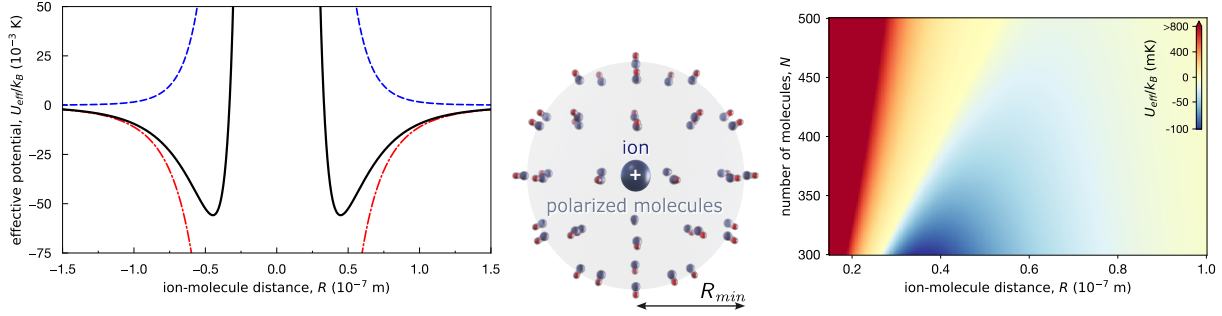


Figure 7. (left panel) Effective radial potential U_{eff}/k_B per particle between a $^{138}\text{Ba}^+$ ion and a quantum gas of $^{23}\text{Na}^{39}\text{K}$ molecules in their rovibronic ground state $|X^1\Sigma^+, v=0, J=0\rangle$ as a function of the ion-molecule distance R . We assume a moderate number density of $n \approx 3 \times 10^{10} \text{ cm}^{-3}$. The balance between attractive ion-neutral (charge-dipole, $\propto R^{-2}$, red dashed-dotted line) and repulsive molecule-molecule (dipole-dipole, $\propto R^{-3}$, blue dashed line) interactions gives rise to a global minimum at R_{min} , suggesting the formation of a polaron-like bound state on a shell at $R_{min} \approx 4.4 \times 10^{-8} \text{ m}$. (center panel) Schematic three-dimensional illustration of a mesoscopic ion-molecule bound state. (right panel) Radial potential U_{eff}/k_B (colorbar in mK) as a function of the molecule number N within the interaction volume V^* . A global minimum (largest negative value of U_{eff}/k_B) is expected for a wide range of N .

would be very strongly confined along the radial direction. The corresponding characteristic dipolar lengths and energies range between $a_{dd} = 1.1 \times 10^{-6} \text{ m} \approx 21100 a_0$ and $E_d/k_B = 40 \text{ nK}$ for $N = 300$ and $a_{dd} = 4.1 \times 10^{-7} \text{ m} \approx 7700 a_0$ and $E_d/k_B = 819 \text{ nK}$ for $N = 500$. These findings based on simplified static considerations provide a first indication that ions immersed into dense quantum gases of polar molecules may lead to the formation of many-body self-bound states (SBS).

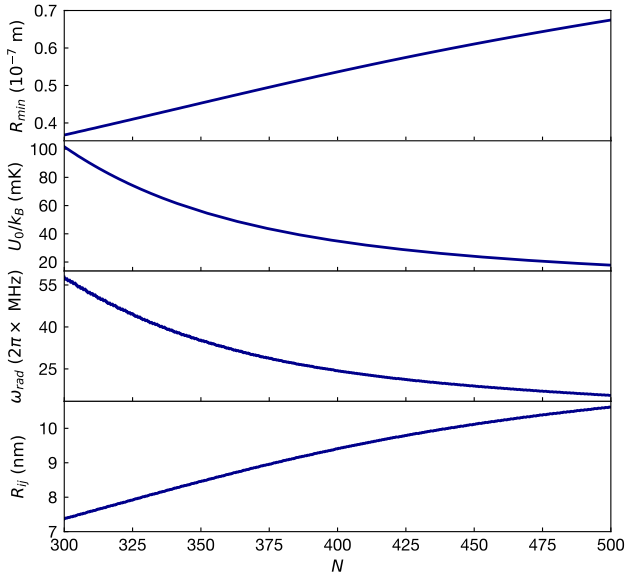


Figure 8. Properties of the self-bound state (SBS) as a function of the number of molecules N in NaK (top to bottom): SBS radius R_{min} , radial potential depth U_0 , secular frequency ω_{rad} , and intermolecular distance R_{ij} .

Another approach to studying quantum-many body phenomena would be to immerse an ion into an ensemble of molecules confined to two dimensions. The latter can be realized, e.g. by utilizing 1D optical standing waves as a periodic trapping potential. In such setups the trapped molecules arrange themselves in layers with a regular spacing typically on the order of the wavelength of the dipole trap λ , as illustrated in Fig.9. This ensures very high trapping frequencies along the axis perpendicular to the trap layers such that the motional degrees of freedom are effectively constrained to a quasi-2D geometry. For an ion positioned at the center of a lattice site, that is for an ion-lattice spacing of $d_{lat} = 0$, we calculate the effective potential of a molecule within the ensemble. As in the case of the 3D gas, we assume that the van der Waals interaction is negligible compared to contributions of \hat{H}_{DD} and \hat{H}_{CD} , which could be achieved by tuning the s-wave scattering length to zero. In this geometry, we obtain $R_{ij} = 2R \sin(\pi/N)$ and $d_{eff}(R) = d(R) \cos(\pi/N)$. Under such conditions, we again find local minima in the effective potential for a wide range of initial molecular densities, e.g. for $N = 40$, where we obtain a well depth of $U_0/k_B = 465 \text{ mK}$, and $R_{min} = 4 \times 10^{-8} \text{ m}$. This indicates the existence of self-bound states in two dimensions.

Many of the discussed properties are reminiscent of polaron-type systems [4–6] and mesoscopic molecular ions [7] which have been studied extensively in the context of ion impurities in an atomic gas, but to the best of our knowledge no experimental realizations have yet been reported. It was suggested that such many-body states may form spontaneously at typical densities of $n = 10^{14} \text{ cm}^{-3}$, with the binding energy being dissipated by phonon emission or by ion-

atom TBR. The drastic enhancement of TBR at such densities would make the observation of mesoscopic molecule-atom states very challenging, but a similar mechanism could be present in both scenarios discussed here, aided by the expected suppression of TBR. Due to the presence of strong dipole-dipole interactions between the molecules, another way to release the binding energy could be by exciting collective surface vibration modes.

Along similar lines, our results suggest that ions embedded in dense polar quantum gases are promising for observing intriguing transitions between, e.g., superfluid, Wigner crystal [95, 96] or supersolid phases [97]. For instance, the predicted quantum phase transition to a crystalline phase with a triangular lattice structure in 2D bosonic dipolar gases requires a dimensionless density of $n_{2D}a_{dd}^2 > 290$ [96]. While this is out of reach in existing contemporary experiments using polar molecules in 1D optical lattices, e.g. fermionic KRb [81], NaK has been suggested as a suitable molecule due to its larger PDM [98] and in the proposed system, an ion-molecule SBS with $N = 350$ yields $n_{2D}a_{dd}^2 > 1.1 \times 10^4$.

6. Ion-mediated shielding of reactive and inelastic collisions

As shown in Fig. 8, typical separations between NaK molecules are $R_{ij} \approx 10$ nm. This is comparable to the characteristic van der Waals length of NaK $\bar{a} \approx 10$ nm [99] and corresponds to strongly increased local densities approaching $n \approx 10^{18}$ cm⁻³. In atom-ion mixtures, such high densities are inaccessible so far due to the extremely short lifetimes resulting from enhanced TBR [23, 25–27] and resonantly enhanced multi-photon ionization (REMPI) [100]. Ensembles of neutral molecules are also known to exhibit two-body and three-body losses with rates close to the universal limit attributed to sticky short-range collisions [35–38]. Since collisional shielding techniques have not been demonstrated for densities in this region, we expect that the molecular ensembles would not be stable without a substantial polarization and the quasi-planar topology of the system.

In the present scenario, the increase of local density is caused by the interaction of the molecules with the electric field of the ion. Due to their increasing alignment in the electric field mutual dipole-dipole repulsion eventually dominates at short range which allows for the formation of stable SBS. In potentials with the extremely high radial harmonic frequencies the bound molecules would be confined to a shell. Due to the topologic similarity of a spherical surface with a planar disc (the corresponding spaces are homeomorphic up to a single point on the sphere),

this confinement to a surface in 3D can be mapped to an equivalent geometry of polar molecules confined in a 2D plane, e.g., in a single site of a 1D optical standing wave. Since the radial electric field of the ion is locally parallel to the normal of any surface element on the shell, the configuration can be described by a homogeneous external electric field perpendicular to the plane containing molecules with individual effective dipole moments aligned parallel to the field and to each other. This situation where head-to-tail collisions are suppressed has been extensively studied with polar molecules, where efficient collisional shielding has been observed in degenerate Fermi gases of KRb [44, 81]. With the large degree of dipole moment alignment predicted for the SBS, we therefore expect highly efficient shielding of two and three-body processes. This should result in a suppression of sticky collisions, three-body losses and REMPI. As all molecules on the shell would be separated from the ion, we also expect that ion-neutral TBR will be efficiently suppressed. Notably, this ion-mediated shielding mechanism persists for or even benefits from very high local densities which are a prerequisite for entering the deep quantum-dominated regime of interactions.

7. Applications of hybrid ion-molecule systems

7.1. Control of collisional processes in molecular gases

Applying sufficiently large homogeneous electric fields along the strongly confining axis has been shown to suppress short-range collisions by preventing head-to-tail collisions [81]. In the proposed ion-molecules experiments a similar arrangement can be realized by replacing the external electric field with a single ion positioned between two lattice sites, as illustrated in Fig. 9. Direct contact between the ion and the molecules would be avoided as long as the ion's position can be controlled on a sub-wavelength scale. This capability was demonstrated in several early works [101, 102]. For a common wavelength of a NIR dipole trap of $\lambda = 1064$ nm, the electric field of an ion displaced by $\lambda/4$, that is, 0.5 of the lowest lattice site spacing, would lead to an equally small induced dipole moment of NaK in two adjacent sites of $0.03 d_0$. Considering the van der Waals potential between two molecules, the effective barrier stemming from induced dipole-dipole repulsion is then $U_0/k_B = 234$ nK $\sim T_{mol}$. This is on the order of the temperature in typical non-degenerate molecular quantum gases such that no significant change of the inelastic collision rate is expected. However, moving the ion closer to a lattice site gives rise to a substantial barrier. As an example, at an ion-lattice site spacing of $d_{lat} = (\lambda/4, \lambda/8, \lambda/16) \approx (133, 66, 33)$ nm the barrier

height increases to $U_0/k_B = (0.06, 6.2, 52.1) \text{ mK} \gg T_{mol}$. This suggests that ion-mediated shielding of short-range collisions may also be achieved using an ion as a nanoscale source of external electric fields without immersing it into the molecular cloud as discussed in section 6. An additional advantage of this approach is that changing d_{lat} , simultaneously lowers the barrier in the adjacent lattice site, e.g. to $U_0/k_B < 10 \text{ nK} \ll T_{mol}$ for $d_{lat} = \lambda/4$ to $\lambda/8$. In this fashion systematic effects between different realizations of an experiment can be reduced allowing for precise differential measurements of the influence of electric fields on the dynamical properties of molecular ensembles such as rates elastic and reactive or sticky collisions.

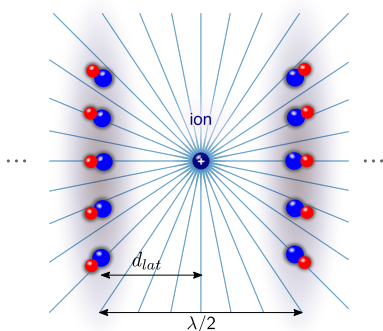


Figure 9. Ion as a high precision source of electric fields. Ba^+ is positioned between the sites of a 1D lattice of NaK ensembles using a Paul trap or an optical dipole trap. The ion-lattice site distance d_{lat} can be controlled with sub-wavelength precision [102].

7.2. Application to quantum technologies

In general, a detailed understanding of solubility processes on the quantum level is of high practical importance, e.g. for the development of drugs. One way to harness the advantage of quantum computation already with the limited computational resources of platforms available today, is to map specific problems onto simplified models that can be implemented on digital quantum simulators [103]. In this context, ions immersed into molecular quantum gases closely resemble atomic cations embedded in a dense polarizable medium, a commonly encountered system. With the expected degree of control this hybrid platform may allow highly precise analog quantum simulations of more complex solubility processes that are currently studied using digital quantum simulators [104].

From the perspective of quantum information processing, atomic ions are among the most performative and advanced platforms in the field [85]. Complementary to these developments, the tremendous progress

achieved in the control over ultracold molecules has also brought forward promising protocols for realizing gate operations by exploiting dipole-dipole interactions [105], or by making use of the internal rotational states and their coupling to microwave fields to implement and manipulate qudits [106]. More recent ideas involve atomic Rydberg atoms to establish and distribute entanglement between molecules [107, 108]. In addition to these prominent examples, hybrid approaches promise to combine the most advantageous properties of different experimental systems. Along these lines, the combination of ions and polar molecules may prove a promising extension to the quantum toolbox of platforms using ions, atoms or molecules. As an example, in comparison to quantum computation protocols based on the interaction between ions and neutral atoms [18], a hybrid approach motivated by early experiments on ion-atom collisions, the long-range interaction between an ion and polar molecules is enhanced by the ratio of their respective static polarizabilities, that is by a factor of typically 10^2 to 10^4 . For instance, at field strength above \mathcal{E}^* corresponding to ion-neutral distances $> 100 \text{ nm}$ the long-range interaction between Ba^+ and NaK is about 3000 times larger than the charge-induced dipole interaction with a Rb atom. These properties may be used to realize ion-molecule interfaces or quantum computation schemes exploiting the dependence of forces exerted on a molecule by an ion on the rotational state of the molecule or the electronic state of the ion, e.g. the S ground state or a Rydberg state.

8. Conclusion

In summary, we have discussed the potential realization of a hybrid ion-molecule system suited for studies of their interactions in the quantum dominated regime. We expect that the combination of currently available techniques and methodology from the fields of ion-atom interactions, in particular bichromatic dipole traps and optimized rf-based hybrid apparatus as well as protocols for the generation of ground-state polar molecules, is feasible within the scope of the envisioned studies. We identify and discuss several promising research directions in different regimes of the molecular ensembles, trap configurations and geometries. Such investigations include reactive inter-species processes with several open channels for chemical reactions and the creation of polyatomic molecular ions. Based on our calculations, we expect that despite the seemingly much higher complexity compared to ion-atom or neutral molecule systems, the additional degrees of freedom, foremost the rotational states of the molecules, can be exploited and controlled to an extent allowing for the realization of tailored schemes for ion-mediated

shielding of reactive molecule-molecule and molecule-ion collisions, as well as sympathetic cooling. Furthermore, we found indications that the interplay between attractive and repulsive interactions induced by the presence of the ion in a dense polar medium facilitates the formation of many-body self-bound states.

These capabilities open the way to access the elusive regime of quantum interactions between ions and neutrals holding great promise to advance several fields and applications including refined control of collisional properties in ensembles of polar molecules, quantum chemistry, quantum-many-body physics, as well as quantum simulations and technologies.

Acknowledgments

L. K. thanks the DFG (German Research Foundation) for support through the Heisenberg Programme — No. 506287139, and Germany’s Excellence Strategy — EXC-2123 QuantumFrontiers — No. 390837967. We are indebted to Mirco Siercke and Silke Ospelkaus for stimulating and insightful discussions. Romain Vexiau is gratefully acknowledged for providing us preliminary data on various diatomic molecules prior to publication.

References

- [1] A. Härter and J. Hecker Denschlag. Cold atom-ion experiments in hybrid traps. *Contemp. Phys.*, 55:33–45, 2014.
- [2] Michał Tomza, Krzysztof Jachymski, Rene Gerritsma, Antonio Negretti, Tommaso Calarco, Zbigniew Idziaszek, and Paul S. Julienne. Cold hybrid ion-atom systems. *Rev. Mod. Phys.*, 91:035001, 2019.
- [3] Rianne S. Lous and René Gerritsma. Ultracold ion-atom experiments: cooling, chemistry, and quantum effects. In Louis F. DiMauro, H el ene Perrin, and Susanne F. Yelin, editors, *Advances in Atomic, Molecular, and Optical Physics*, volume 71 of *Advances In Atomic, Molecular, and Optical Physics*, pages 65–133. Academic Press, 2022.
- [4] J. Goold, H. Doerk, Z. Idziaszek, T. Calarco, and Th. Busch. Ion-induced density bubble in a strongly correlated one-dimensional gas. *Phys. Rev. A*, 81:041601, 2010.
- [5] J. M. Schurer, A. Negretti, and P. Schmelcher. Unraveling the Structure of Ultracold Mesoscopic Molecular Ions. *Phys. Rev. Lett.*, 063001:1–6, 2017.
- [6] Grigory E. Astrakharchik, Luis A. Pe a Ardila, Krzysztof Jachymski, and Antonio Negretti. Many-body bound states and induced interactions of charged impurities in a bosonic bath. *Nat. Commun.*, 14:1647, 2023.
- [7] R. C ot e, V. Kharchenko, and M D Lukin. Mesoscopic Molecular Ions in Bose-Einstein Condensates. *Phys. Rev. Lett.*, 89:093001, 2002.
- [8] R. C ot e. From classical mobility to hopping conductivity: charge hopping in an ultracold gas. *Phys. Rev. Lett.*, 85:5316–9, 2000.
- [9] T. Dieterle, M. Berngruber, C. H olz, R. L ow, K. Jachymski, T. Pfau, and F. Meinert. Transport of a Single Cold Ion Immersed in a Bose-Einstein Condensate. *Phys. Rev. Lett.*, 126:33401, 2021.
- [10] U. Bissbort, D. Cocks, A. Negretti, Z. Idziaszek, T. Calarco, F. Schmidt-Kaler, W. Hofstetter, and R. Gerritsma. Emulating Solid-State Physics with a Hybrid System of Ultracold Ions and Atoms. *Phys. Rev. Lett.*, 111:080501, 2013.
- [11] R. Gerritsma, A. Negretti, H. Doerk, Z. Idziaszek, T. Calarco, and F. Schmidt-Kaler. Bosonic Josephson junction controlled by a single trapped ion. *Phys. Rev. Lett.*, 109:1–5, 2012.
- [12] Winthrop W. Smith, Oleg P. Makarov, and Jian Lin. Cold ion-neutral collisions in a hybrid trap. *J. Mod. Opt.*, 52:2253–2260, 2005.
- [13] Andrew T. Grier, Marko Cetina, Fedja Oru evi c, and Vladan Vuleti c. Observation of Cold Collisions between Trapped Ions and Trapped Atoms. *Phys. Rev. Lett.*, 102:223201, 2009.
- [14] Christoph Zipkes, Stefan Palzer, Lothar Ratschbacher, Carlo Sias, and Michael K ohl. Cold Heteronuclear Atom-Ion Collisions. *Phys. Rev. Lett.*, 105:133201, 2010.
- [15] Stefan Willitsch, Martin T. Bell, Alexander D. Gingell, Simon R. Procter, and Timothy P. Softley. Cold Reactive Collisions between Laser-Cooled Ions and Velocity-Selected Neutral Molecules. *Phys. Rev. Lett.*, 100:043203, 2008.
- [16] Wade G. Rellergert, Scott T. Sullivan, Svetlana Kotochigova, Alexander Petrov, Kuang Chen, Steven J. Schowalter, and Eric R. Hudson. Measurement of a Large Chemical Reaction Rate between Ultracold Closed-Shell ^{40}Ca Atoms and Open-Shell ^{174}Yb Ions Held in a Hybrid Atom-Ion Trap. *Phys. Rev. Lett.*, 107:243201, 2011.
- [17] Pascal Weckesser, Fabian Thielemann, Dariusz Wiater, Agata Wojciechowska, Leon Karpa, Krzysztof Jachymski, Michał Tomza, Thomas Walker, and Tobias Schaetz. Observation of Feshbach resonances between a single ion and ultracold atoms. *Nature*, 600:429–433, 2021.
- [18] Hauke Doerk, Zbigniew Idziaszek, and Tommaso Calarco. Atom-ion quantum gate. *Phys. Rev. A*, 81:012708, 2010.
- [19] T. Secker, R. Gerritsma, A. W. Glaetzle, and A. Negretti. Controlled long-range interactions between rydberg atoms and ions. *Phys. Rev. A*, 94:013420, 2016.
- [20] Mostafa R. Ebgha, Shahpoor Saeidian, Peter Schmelcher, and Antonio Negretti. Compound atom-ion josephson junction: Effects of finite temperature and ion motion. *Phys. Rev. A*, 100:033616, 2019.
- [21] J. Schmidt, P. Weckesser, F. Thielemann, T. Schaetz, and L. Karpa. Optical Traps for Sympathetic Cooling of Ions with Ultracold Neutral Atoms. *Phys. Rev. Lett.*, 124:53402, 2020.
- [22] T. Feldker, H. F urst, H. Hirzler, N. V. Ewald, M. Mazzanti, D. Wiater, M. Tomza, and R. Gerritsma. Buffer gas cooling of a trapped ion to the quantum regime. *Nat. Phys.*, 16:413–416, 2020.
- [23] Arne H arter, Artjom Kr ukow, Andreas Brunner, Wolfgang Schnitzler, Stefan Schmid, and Johannes Hecker Denschlag. Single Ion as a Three-Body Reaction Center in an Ultracold Atomic Gas. *Phys. Rev. Lett.*, 109:123201, 2012.
- [24] Amir Mohammadi, Artjom Kr ukow, Amir Mahdian, Markus Deiß, Jes us P erez-R ıos, Humberto Da Silva, Maurice Raoult, Olivier Dulieu, and Johannes Hecker Denschlag. Life and death of a cold BaRb^+ molecule inside an ultracold cloud of Rb atoms. *Phys. Rev. Research*, 3:13196, 2021.
- [25] Artjom Kr ukow, Amir Mohammadi, Arne H arter, Johannes Hecker Denschlag, Jes us P erez-R ıos, and Chris H Greene. Energy Scaling of Cold Atom-Atom-

- Ion Three-Body Recombination. *Phys. Rev. Lett.*, 116:193201, 2016.
- [26] T. Dieterle, M. Berngruber, C. Hölzl, R. Löw, K. Jachymski, T. Pfau, and F. Meinert. Inelastic collision dynamics of a single cold ion immersed in a Bose-Einstein condensate. *Phys. Rev. A*, 102:041301, Oct 2020.
- [27] Amrendra Pandey, Romain Vexiau, Luis Gustavo Marcassa, Olivier Dulieu, and Nadia Bouloufa-Maafa. Ultracold charged atom-dimer collisions: state-selective charge exchange and three-body recombination [Preprint]. Available from: <https://doi.org/10.48550/arxiv.2407.14824>, 2024.
- [28] Marko Cetina, Andrew T. Grier, and Vladan Vuletić. Micromotion-Induced Limit to Atom-Ion Sympathetic Cooling in Paul Traps. *Phys. Rev. Lett.*, 109:253201, 2012.
- [29] K. S. Kleinbach, Felix Engel, Thomas Dieterle, Robert Löw, Tilman Pfau, and Florian Meinert. Ionic Impurity in a Bose-Einstein Condensate at Submicrokelvin Temperatures. *Phys. Rev. Lett.*, 120:193401, 2018.
- [30] Nicolas Zuber, Viraatt S. V. Anasuri, Moritz Berngruber, Yi-Quan Zou, Florian Meinert, Robert Löw, and Tilman Pfau. Observation of a molecular bond between ions and Rydberg atoms. *Nature*, 605:453–456, 2022.
- [31] T. Secker, N. Ewald, J. Joger, H. Fürst, T. Feldker, and R. Gerritsma. Trapped Ions in Rydberg-Dressed Atomic Gases. *Phys. Rev. Lett.*, 118:263201, 2017.
- [32] Leon Karpa. Interactions of ions and ultracold neutral atom ensembles in composite optical dipole traps: Developments and perspectives. *Atoms*, 9:39, 2021.
- [33] S. Ospelkaus, K.-K. Ni, D. Wang, M. H.G. G. de Miranda, B. Neyenhuis, G. Quémener, P. S. Julienne, J. L. Bohn, D. S. Jin, and J. Ye. Quantum-State Controlled Chemical Reactions of Ultracold Potassium-Rubidium Molecules. *Science*, 327:853–857, 2010.
- [34] K. K. Ni, S. Ospelkaus, M. H.G. De Miranda, A. Pe'er, B. Neyenhuis, J. J. Zirbel, S. Kotochigova, P. S. Julienne, D. S. Jin, and J. Ye. A high phase-space-density gas of polar molecules. *Science*, 322:231–235, 2008.
- [35] James F. E. Croft, John L. Bohn, and Goulven Quémener. Anomalous lifetimes of ultracold complexes decaying into a single channel. *Phys. Rev. A*, 107:023304, 2023.
- [36] Krzysztof Jachymski, Marcin Gronowski, and Michał Tomza. Collisional losses of ultracold molecules due to intermediate complex formation. *Phys. Rev. A*, 106:L041301, 2022.
- [37] Michael Mayle, Goulven Quémener, Brandon P. Ruzic, and John L. Bohn. Scattering of ultracold molecules in the highly resonant regime. *Phys. Rev. A*, 87:012709, 2013.
- [38] Arthur Christianen, Tijs Karman, and Gerrit C. Groenenboom. Quasiclassical method for calculating the density of states of ultracold collision complexes. *Phys. Rev. A*, 100:032708, 2019.
- [39] A. V. Gorshkov, P. Rabl, G. Pupillo, A. Micheli, P. Zoller, M. D. Lukin, and H. P. Büchler. Suppression of inelastic collisions between polar molecules with a repulsive shield. *Phys. Rev. Lett.*, 073201:1–4, 2008.
- [40] Goulven Quémener and John L. Bohn. Dynamics of ultracold molecules in confined geometry and electric field. *Phys. Rev. A*, 83:012705, 2011.
- [41] Tijs Karman and Jeremy M. Hutson. Microwave shielding of ultracold polar molecules with imperfectly circular polarization. *Phys. Rev. A*, 100:052704, 2019.
- [42] T Xie, M Lepers, R Vexiau, A Orbán, O Dulieu, and N. Bouloufa-Maafa. Optical Shielding of Destructive Chemical Reactions between Ultracold Ground-State NaRb Molecules. *Phys. Rev. Lett.*, 125:153202, 2020.
- [43] Charbel Karam, Romain Vexiau, Nadia Bouloufa-Maafa, Olivier Dulieu, Maxence Lepers, Mara Meyer zum Alten Borgloh, Silke Ospelkaus, and Leon Karpa. Two-photon optical shielding of collisions between ultracold polar molecules. *Phys. Rev. Research*, 5:033074, 2023.
- [44] Kyle Matsuda, Luigi De Marco, Jun Ru Li, William G. Tobias, Giacomo Valtolina, Goulven Quémener, and Jun Ye. Resonant collisional shielding of reactive molecules using electric fields. *Science*, 370:1324–1327, 2020.
- [45] Loïc Anderegg, Sean Burchesky, Yicheng Bao, Scarlett S Yu, Tijs Karman, Eunmi Chae, Kang-Kuen Ni, Wolfgang Ketterle, and John M. Doyle. Observation of microwave shielding of ultracold molecules. *Science*, 373:779–782, 2021.
- [46] Andreas Schindewolf, Roman Bause, Xing-Yan Chen, Marcel Duda, Tijs Karman, Immanuel Bloch, and Xin-Yu Luo. Evaporation of microwave-shielded polar molecules to quantum degeneracy. *Nature*, 607:677–681, 2022.
- [47] Junyu Lin, Guanghua Chen, Mucan Jin, Zhaopeng Shi, Fulin Deng, Wenxian Zhang, Goulven Quémener, Tao Shi, Su Yi, and Dajun Wang. Microwave shielding of bosonic diatomic molecules. *Phys. Rev. X*, 13:031032, 2023.
- [48] Niccolò Bigagli, Weijun Yuan, Siwei Zhang, Boris Bulatovic, Tijs Karman, Ian Stevenson, and Sebastian Will. Observation of Bose-Einstein condensation of dipolar molecules. *Nature*, 631:289–293, 2024.
- [49] Luigi De Marco, Giacomo Valtolina, Kyle Matsuda, William G Tobias, Jacob P Covey, and Jun Ye. A degenerate Fermi gas of polar molecules. *Science*, 363:853–856, 2019.
- [50] Stefan Schmid, Arne Härter, and Johannes Hecker Denschlag. Dynamics of a Cold Trapped Ion in a Bose-Einstein Condensate. *Phys. Rev. Lett.*, 105:133202, 2010.
- [51] K Ravi, Seunghyun Lee, Arijit Sharma, G Werth, and S.A. Rangwala. Cooling and stabilization by collisions in a mixed ion-atom system. *Nat. Commun.*, 3:1126, 2012.
- [52] Felix H.J. Hall, Pascal Eberle, Gregor Hegi, Maurice Raoult, Mireille Aymar, Olivier Dulieu, and Stefan Willitsch. Ion-neutral chemistry at ultralow energies: dynamics of reactive collisions between laser-cooled Ca⁺ ions and Rb atoms in an ion-atom hybrid trap. *Mol. Phys.*, 111:2020–2032, 2013.
- [53] Shinsuke Haze, Mizuki Sasakawa, Ryoichi Saito, Ryosuke Nakai, and Takashi Mukaiyama. Cooling Dynamics of a Single Trapped Ion via Elastic Collisions with Small-Mass Atoms. *Phys. Rev. Lett.*, 120:043401, 2018.
- [54] Ziv Meir, Tomas Sikorsky, Ruti Ben-shlomi, Nitzan Akerman, Yehonatan Dallal, and Roei Ozeri. Dynamics of a Ground-State Cooled Ion Colliding with Ultracold Atoms. *Phys. Rev. Lett.*, 117:243401, 2016.
- [55] J. Deiglmayr, A. Göritz, T. Best, M. Weidemüller, and R. Wester. Reactive collisions of trapped anions with ultracold atoms. *Phys. Rev. A*, 86:043438, 2012.
- [56] Bubai Rahaman, Satyabrata Baidya, and Sourav Dutta. A versatile apparatus for simultaneous trapping of multiple species of ultracold atoms and ions to enable studies of low energy collisions and cold chemistry. *J. Chem. Phys.*, 160, 2024.
- [57] Leon Karpa. *Trapping Single Ions and Coulomb Crystals with Light Fields*. SpringerBriefs in Physics. Springer International Publishing, Cham, 2019.
- [58] Jessie T. Zhang, Lewis R B Picard, William B. Cairncross, Kenneth Wang, Yichao Yu, Fang Fang, and Kang-Kuen Ni. An optical tweezer array of ground-state polar molecules. *Quantum Sci. Technol.*, 7:035006, 2022.
- [59] Philip D. Gregory, Luke M. Fernley, Albert Li Tao, Sarah L. Bromley, Jonathan Stepp, Zewen Zhang, Svetlana Kotochigova, Kaden R. A. Hazzard, and

- Simon L. Cornish. Second-scale rotational coherence and dipolar interactions in a gas of ultracold polar molecules. *Nat. Phys.*, 20:415–421, 2024.
- [60] Nathaniel B. Vilas, Paige Robichaud, Christian Hallas, Grace K. Li, Loïc Anderegg, and John M. Doyle. An optical tweezer array of ultracold polyatomic molecules. *Nature*, 628:282–286, 2024.
- [61] Connor M. Holland, Yukai Lu, and Lawrence W. Cheuk. Bichromatic imaging of single molecules in an optical tweezer array. *Phys. Rev. Lett.*, 131:053202, 2023.
- [62] H. J. Williams, L. Caldwell, N. J. Fitch, S. Truppe, J. Rodewald, E. A. Hinds, B. E. Sauer, and M. R. Tarbutt. Magnetic trapping and coherent control of laser-cooled molecules. *Phys. Rev. Lett.*, 120:163201, 2018.
- [63] Loïc Anderegg, Lawrence W. Cheuk, Yicheng Bao, Sean Burchesky, Wolfgang Ketterle, Kang-Kuen Ni, and John M. Doyle. An optical tweezer array of ultracold molecules. *Science*, 365:1156–1158, 2019.
- [64] Marian Rockenhäuser, Felix Kogel, Tatsam Garg, Sebastián A. Morales-Ramírez, and Tim Langen. Laser cooling of barium monofluoride molecules using synthesized optical spectra, 2024.
- [65] Debayan Mitra, Nathaniel B. Vilas, Christian Hallas, Loïc Anderegg, Benjamin L. Augenbraun, Louis Baum, Calder Miller, Shivam Raval, and John M. Doyle. Direct laser cooling of a symmetric top molecule. *Science*, 369:1366–1369, 2020.
- [66] Kai K. Voges, Philipp Gersema, Mara Meyer zum Alten Borgloh, Torben A. Schulze, Torsten Hartmann, Alessandro Zenesini, and Silke Ospelkaus. Ultracold gas of bosonic $\text{Na}^{23}\text{K}^{39}$ ground-state molecules. *Phys. Rev. Lett.*, 125:083401, 2020.
- [67] Thomas Huber, Alexander Lambrecht, Julian Schmidt, Leon Karpa, and Tobias Schaetz. A far-off-resonance optical trap for a Ba^+ ion. *Nat. Commun.*, 5:5587, 2014.
- [68] Alexander Lambrecht, Julian Schmidt, Pascal Weckesser, Markus Debatin, Leon Karpa, and Tobias Schaetz. Long lifetimes and effective isolation of ions in optical and electrostatic traps. *Nat. Photonics*, 11:704–707, 2017.
- [69] Julian Schmidt, Alexander Lambrecht, Pascal Weckesser, Markus Debatin, Leon Karpa, and Tobias Schaetz. Optical Trapping of Ion Coulomb Crystals. *Phys. Rev. X*, 8:021028, 2018.
- [70] Daniel Hoenig, Fabian Thielemann, Leon Karpa, Thomas Walker, Amir Mohammadi, and Tobias Schaetz. Trapping Ion Coulomb Crystals in an Optical Lattice. *Phys. Rev. Lett.*, 132:133003, 2024.
- [71] Rudolf Grimm, Matthias Weidemüller, and Yurii B. Ovchinnikov. Optical dipole traps for neutral atoms. volume 42 of *Advances In Atomic, Molecular, and Optical Physics*, pages 95–170. Academic Press, 2000.
- [72] R. Vexiau, D Borsalino, M Lepers, A Orbán, M Aymar, and O Dulieu. Dynamic dipole polarizabilities of heteronuclear alkali dimers : optical response , trapping and control of ultracold molecules. *Int. Rev. Phys. Chem.*, 36:541–620, 2017.
- [73] Roman Bause, Ming Li, Andreas Schindewolf, Xing-Yan Chen, Marcel Duda, Svetlana Kotochigova, Immanuel Bloch, and Xin-Yu Luo. Tune-out and magic wavelengths for ground-state $^{23}\text{Na}^{40}\text{K}$ molecules. *Phys. Rev. Lett.*, 125:023201, 2020.
- [74] Pascal Weckesser, Fabian Thielemann, Daniel Hoenig, Alexander Lambrecht, Leon Karpa, and Tobias Schaetz. Trapping, shaping, and isolating of an ion Coulomb crystal via state-selective optical potentials. *Phys. Rev. A*, 103:013112, 2021.
- [75] J. Aldegunde, Ben A. Rivington, Piotr S. Żuchowski, and Jeremy M. Hutson. Hyperfine energy levels of alkali-metal dimers: Ground-state polar molecules in electric and magnetic fields. *Phys. Rev. A*, 78:033434, 2008.
- [76] J. L. Dunham. The energy levels of a rotating vibrator. *Phys. Rev.*, 41:721–731, 1932.
- [77] R. Côté and A. Dalgarno. Ultracold atom-ion collisions. *Phys. Rev. A*, 62:012709, 2000.
- [78] P. Langevin. A fundamental formula of kinetic theory. *Ann. Chim. Phys.*, 5:245, 1905.
- [79] H. J. Metcalf and P. van der Straten. *Laser Cooling and Trapping*. Springer-Verlag, New York, 1999.
- [80] J. Pérez-Ríos. Cold chemistry: a few-body perspective on impurity physics of a single ion in an ultracold bath. *Mol. Phys.*, 119:e1881637, 2021.
- [81] Giacomo Valtolina, Kyle Matsuda, William G. Tobias, Jun Ru Li, Luigi De Marco, and Jun Ye. Dipolar evaporation of reactive molecules to below the Fermi temperature. *Nature*, 588:239–243, 2020.
- [82] J. Joger, H. FÜRST, N. Ewald, T. Feldker, M. Tomza, and R. Gerritsma. Observation of collisions between cold Li atoms and Yb^+ ions. *Phys. Rev. A*, 96:030703, 2017.
- [83] N. V. Ewald, T. Feldker, H. Hirzler, H. A. FÜRST, and R. Gerritsma. Observation of Interactions between Trapped Ions and Ultracold Rydberg Atoms. *Phys. Rev. Lett.*, 122:253401, 2019.
- [84] M.-G. Hu, Y. Liu, D. D. Grimes, Y.-W. Lin, A. H. Gheorghe, R. Vexiau, N. Bouloufa-Maafa, O. Dulieu, T. Rosenband, and K.-K. Ni. Direct observation of bimolecular reactions of ultracold KRb molecules. *Science*, 366:1111–1115, 2019.
- [85] D. Leibfried, R. Blatt, C. Monroe, and D. Wineland. Quantum dynamics of single trapped ions. *Rev. Mod. Phys.*, 75:281–324, 2003.
- [86] Julian Schmidt, Daniel Hoenig, Pascal Weckesser, Fabian Thielemann, Tobias Schaetz, and Leon Karpa. Mass-selective removal of ions from Paul traps using parametric excitation. *Appl. Phys. B*, 126:176, 2020.
- [87] Prateek Puri, Michael Mills, Christian Schneider, Ionel Simbotin, John A. Montgomery, Robin Côté, Arthur G. Suits, and Eric R. Hudson. Synthesis of mixed hypermetallic oxide BaOCa^+ from laser-cooled reagents in an atom-ion hybrid trap. *Science*, 357:1370–1375, 2017.
- [88] Ziv Meir, Meirav Pinkas, Tomas Sikorsky, Ruti Ben-Shlomi, Nitzan Akerman, and Roei Ozeri. Direct Observation of Atom-Ion Nonequilibrium Sympathetic Cooling. *Phys. Rev. Lett.*, 121:53402, 2018.
- [89] Ziv Meir, Tomas Sikorsky, Nitzan Akerman, Ruti Ben-Shlomi, Meirav Pinkas, and Roei Ozeri. Single-shot energy measurement of a single atom and the direct reconstruction of its energy distribution. *Phys. Rev. A*, 96:020701, 2017.
- [90] Fabian Wolf, Yong Wan, Jan C. Heip, Florian Gebert, Chunyan Shi, and Piet O. Schmidt. Non-destructive state detection for quantum logic spectroscopy of molecular ions. *Nature*, 530:457–460, 2016.
- [91] Mudit Sihal, Ziv Meir, Kaveh Najafian, Gregor Hegi, and Stefan Willitsch. Quantum-nondemolition state detection and spectroscopy of single trapped molecules. *Science*, 367:1213–1218, 2020.
- [92] M. Aymar and O. Dulieu. Calculation of accurate permanent dipole moments of the lowest $1,3\Sigma^+$ states of heteronuclear alkali dimers using extended basis sets. *J. Chem. Phys.*, 122:204302, 2005.
- [93] R. Guérou, M. Aymar, and O. Dulieu. Ground state of the polar alkali-metal-atom-strontium molecules: Potential energy curve and permanent dipole moment. *Phys. Rev. A*, 82:042508, 2010.
- [94] H. Hirzler, R. S. Lous, E. Trimby, J. Pérez-Ríos, A. Safavi-Naini, and R. Gerritsma. Observation of chemical

- reactions between a trapped ion and ultracold feshbach dimers. *Phys. Rev. Lett.*, 128:103401, 2022.
- [95] H. P. Büchler, E. Demler, M. Lukin, A. Micheli, N. Prokof'ev, G. Pupillo, and P. Zoller. Strongly correlated 2d quantum phases with cold polar molecules: Controlling the shape of the interaction potential. *Phys. Rev. Lett.*, 98:060404, 2007.
- [96] G. E. Astrakharchik, J. Boronat, I. L. Kurbakov, and Yu. E. Lozovik. Quantum phase transition in a two-dimensional system of dipoles. *Phys. Rev. Lett.*, 98:060405, 2007.
- [97] Matthias Schmidt, Lucas Lassablière, Goulven Quémener, and Tim Langen. Self-bound dipolar droplets and supersolids in molecular Bose-Einstein condensates. *Phys. Rev. Research*, 4:1–14, 2022.
- [98] N. Matveeva and S. Giorgini. Liquid and crystal phases of dipolar fermions in two dimensions. *Phys. Rev. Lett.*, 109:200401, 2012.
- [99] Paul S. Julienne, Thomas M. Hanna, and Zbigniew Idziaszek. Universal ultracold collision rates for polar molecules of two alkali-metal atoms. *Phys. Chem. Chem. Phys.*, 13:19114–19124, 2011.
- [100] A. Härter, A. Krüchow, M. Deiß, B. Drews, E. Tiemann, and J. Hecker Denschlag. Population distribution of product states following three-body recombination in an ultracold atomic gas. *Nat. Phys.*, 9:512–517, 2013.
- [101] G. R. Guthöhrlein, M. Keller, Kazuhiro Hayasaka, Walther Lange, and Herbert Walther. A single ion as a nanoscopic probe of an optical field. *Nature*, 414:49–51, 2001.
- [102] Leon Karpa, Alexei Bylinskii, Dorian Gangloff, Marko Cetina, and Vladan Vuletić. Suppression of Ion Transport due to Long-Lived Subwavelength Localization by an Optical Lattice. *Phys. Rev. Lett.*, 111:163002, 2013.
- [103] Andrew J. Daley, Immanuel Bloch, Christian Kokail, Stuart Flannigan, Natalie Pearson, Matthias Troyer, and Peter Zoller. Practical quantum advantage in quantum simulation. *Nature*, 607:667–676, 2022.
- [104] Davide Castaldo, Soran Jahangiri, Alain Delgado, and Stefano Corni. Quantum simulation of molecules in solution. *J. Chem. Theory Comput.*, 18:7457–7469, 2022. PMID: 36351289.
- [105] D. DeMille. Quantum Computation with Trapped Polar Molecules. *Phys. Rev. Lett.*, 88:067901, 2002.
- [106] Rahul Sawant, Jacob A. Blackmore, Philip D. Gregory, Jordi Mur-Petit, Dieter Jaksch, Jesús Aldegunde, Jeremy M. Hutson, M. R. Tarbutt, and Simon L. Cornish. Ultracold polar molecules as qudits. *New J. Phys.*, 22:013027, 2020.
- [107] Chi Zhang and M. R. Tarbutt. Quantum Computation in a Hybrid Array of Molecules and Rydberg Atoms. *PRX Quantum*, 3:1, 2022.
- [108] Kenneth Wang, Conner P. Williams, Lewis R.B. Picard, Norman Y. Yao, and Kang-Kuen Ni. Enriching the quantum toolbox of ultracold molecules with rydberg atoms. *PRX Quantum*, 3:030339, 2022.